Chapter

Improved Direct Torque Control Based on Neural Network of the Double-Star Induction Machine Using Deferent Multilevel Inverter

Mohamed Haithem Lazreg and Abderrahim Bentaallah

Abstract

In this chapter, we will compare the performance of a multilevel direct torque control (DTC) control for the double-star induction machine (DSIM) based on artificial neural network (ANN). The application of DTC control brings a very interesting solution to the problems of robustness and dynamics. However, this control has some disadvantages such as variable switching frequency, size, and complexity of the switching tables and the strong ripple torque. A solution to this problem is to increase the output voltage level of the inverter and associate the DTC control with modern control techniques such as artificial neural networks. Theoretical elements and simulation results are presented and discussed. As results, the flux and torque ripple of the five-level DTC-ANN control significantly reduces compared to the flux and torque ripple of the three-level DTC-ANN control. By viewing the simulation results using MATLAB/Simulink for both controls, the results obtained showed a very satisfactory behavior of this machine.

Keywords: double-star induction machine (DSIM), direct torque control (DTC), three-level inverter, five-level inverter, artificial neural network (ANN)

1. Introduction

The use of a conventional two-level inverter in the field of high power applications is not appropriate because it requires electronic components capable of withstanding high reverse voltage and high current. Another disadvantage of this inverter is the problem of magnetic interference caused by the abrupt change of the output voltage of the inverter from zero to high value [1].

With the appearance of the structures of the multilevel inverters proposed for the first time by [2], the research was able to face the handicaps presented by the classical structure. The goal of this research focus is to improve the quality of the output voltage, as well as to overcome the problems associated with two-level inverters. There are several topologies of multilevel inverters such as floating-diode, floating-capacitor, and cascaded inverters [3]. These structures make it possible to generate an output voltage of several levels.

Diode-clamped inverter (DCI) is the one that attracts the most attention because of the simplicity of its structure compared to the floating capacity inverter; in fact

we do not need to use capacities for each phase, which eliminates the risks of parasitic resonances [4]. In this structure, diodes called floating diodes are associated with each phase, which serves to apply the different voltage levels of the DC source.

In high power, AC machines powered by static inverters find more and more applications. But the constraints on the power components limit the switching frequency and therefore the performance. To enable the use of higher switching frequency components, the power must be divided. To do this, one of the solutions is to use multiphase machines thanks to their advantages, such as the power segmentation and the minimization of the ripples of the torque (elimination of the harmonic torque of rank six). One of the most common examples of multiphase machines is the double-star induction machine (DSIM) [5].

To improve the decoupling between the flux and the torque, a so-called direct torque control (DTC) control technique has been applied.

The conventional direct torque control (DTCc) is proposed by Takahashi and Depenbrock in 1985 [2], and several studies allowed to apply this control technique on multiphase machines. As for each control, the DTC has advantages and disadvantages, and among these advantages, the stator resistance is theoretically the only parameter of the machine that intervenes in the control. This is essential for estimating the stator flux vector [6]. From this purely theoretical point of view, one can thus consider a great robustness compared to the other parameters of the machine; the block PWM is usually deleted [7].

Despite these advantages, this control also has significant disadvantages, the problem of instability such as the lack of control of the generator of acoustic noise at the machine. In addition, the use of hysteresis tapes is the cause of electromagnetic torque ripples and noise in the machine. To solve these drawbacks, in the framework of this work, we try to apply the multilevel direct torque control for DSIM and to develop a new control method such as artificial neural networks that replaces the switching tables [8].

This chapter is organized as follows: the DSIM model will be presented in the next section. The three-level and the five-level inverter modeling is described in the third and fourth section. The control method by DTC based on artificial neural networks (DTC-ANN) will be discussed in the fifth section. Moreover, in the sixth section, the simulation results are presented. Finally, a general conclusion summarizes this work.

2. DSIM model

In the conventional configuration, two identical three-phase windings share the same stator and are shifted by an electric angle of 30°. The rotor structure remains identical to that of a three-phase machine [9].

The model of machine DSIM is nonlinear. The DSIM model fed by voltage inverter is given by the following equations [10]:

$$\frac{dX}{dt} = AX + BU \tag{1}$$

$$T_{em} = p\frac{L_m}{L_r + L_m}\left[\varphi_{dr}\left(i_{qs1} + i_{qs2}\right) - \varphi_{qr}\left(i_{ds1} + i_{ds2}\right)\right] \tag{2}$$

$$J\frac{d\Omega}{dt} = T_{em} - T_L - k_f\Omega \tag{3}$$

where:

$$X = [x_1, x_2, x_3, x_4, x_5, x_6]^T = \left[i_{ds1}, i_{ds2}, i_{qs1}, i_{qs2}, \phi_{dr}, \phi_{qr}\right]^T$$

$$U = \left[v_{ds1}, v_{ds2}, v_{qs1}, v_{qs2}\right]$$

Matrixes A and B are given by

$$A = \begin{bmatrix} a_1 & a_2 & a_3 & a_4 & a_5 & a_6 \\ -a_2 & a_1 & -a_4 & a_3 & -a_6 & a_5 \\ a_3 & a_4 & a_1 & a_2 & a_5 & a_6 \\ -a_4 & a_3 & -a_2 & a_1 & -a_6 & a_5 \\ a_9 & a_8 & a_7 & 0 & a_7 & 0 \\ -a_8 & a_9 & 0 & a_7 & 0 & a_7 \end{bmatrix} \quad B = \begin{bmatrix} b_1 & 0 & b_2 & 0 \\ 0 & b_1 & 0 & b_2 \\ b_2 & 0 & b_1 & 0 \\ 0 & b_2 & 0 & b_1 \end{bmatrix}$$

where

$$a_1 = b_0 \frac{L_m}{T_r} - b_1 R_s,\ a_2 = \omega_s(b_1 L_1 + b_2 L_2),\ a_3 = b_0 \frac{L_m}{T_r} - b_2 R_s,\ a_4 = \omega_s(b_1 L_2 + b_2 L_1),$$
$$a_5 = \frac{-b_0}{T_r},\ a_6 = a_0 b_3 + \omega_g b_0,\ a_7 = \frac{L_m}{T_r},\ a_8 = \omega_g,\ a_9 = -\frac{1}{T_r},\ a_{10} = \frac{3}{2} p \frac{L_m}{L_r},$$
$$\sigma = 1 - \frac{L_m^2}{L_s L_r},\ L_1 = \sigma L_s, L_2 = \sigma L_s - l_s, L_3 = L_s(1-\sigma),\ a_0 = \frac{L_m}{L_r},\ b_0 = \frac{L_m}{L_r(L_1 + L_2)},$$
$$b_1 = \frac{L_1}{L_1^2 - L_2^2},\ b_2 = \frac{L_2}{L_1^2 - L_2^2},\ b_3 = \omega_s(b_1 + b_2)$$

3. Modeling of three-level inverter

Figure 1 shows the structure of the three-level floating-diode inverter introduced by A. Nabae and H. Akagi in 1981 [11] (**Table 1**).

The three symmetrical arms consist of four fully controllable switches. These switches must not be opened or closed simultaneously, in order to avoid short circuiting of the DC source at the input of the inverter. Each switch is composed of an antiparallel transistor with a diode. The floating diodes ensure the application of the different voltage levels at the output of each arm. The DC input voltage is divided into two equal parts by using two capacitors. Each capacitor must be sized for a voltage equal to $v_{dc}/2$ [12].

The switching function of each switch T_{xki} (k = 1, 2, i = 1 ... 4, x = a, b, and c) is defined as follows:

$$F_{xki} = \begin{cases} 1 \text{ if } T_{xki} \text{ is ON} \\ 0 \text{ if } T_{xki} \text{ is OFF} \end{cases} \tag{4}$$

The controls of the switches of the lower half-arms are complementary to those of the upper half-arms:

$$F_{xki} = 1 - F_{xk(i-2)} \tag{5}$$

For each arm, we define three connection functions:

$$\begin{cases} F_{c1xk} = F_{c1xk}F_{c2xk} \\ F_{c2xk} = F_{c2xk}F_{c3xk} \\ F_{c3xk} = F_{c3xk}F_{c4xk} \end{cases} \quad (6)$$

The output voltages with respect to the neutral point of the DC source are expressed by

$$\begin{pmatrix} v_{a0k} \\ v_{b0k} \\ v_{c0k} \end{pmatrix} = \begin{pmatrix} F_{c1ak} & F_{c2ak} & F_{c3ak} \\ F_{c1bk} & F_{c2bk} & F_{c3bk} \\ F_{c1ck} & F_{c2ck} & F_{c3ck} \end{pmatrix} \begin{pmatrix} v_{c2} \\ 0 \\ -v_{c1} \end{pmatrix} \quad (7)$$

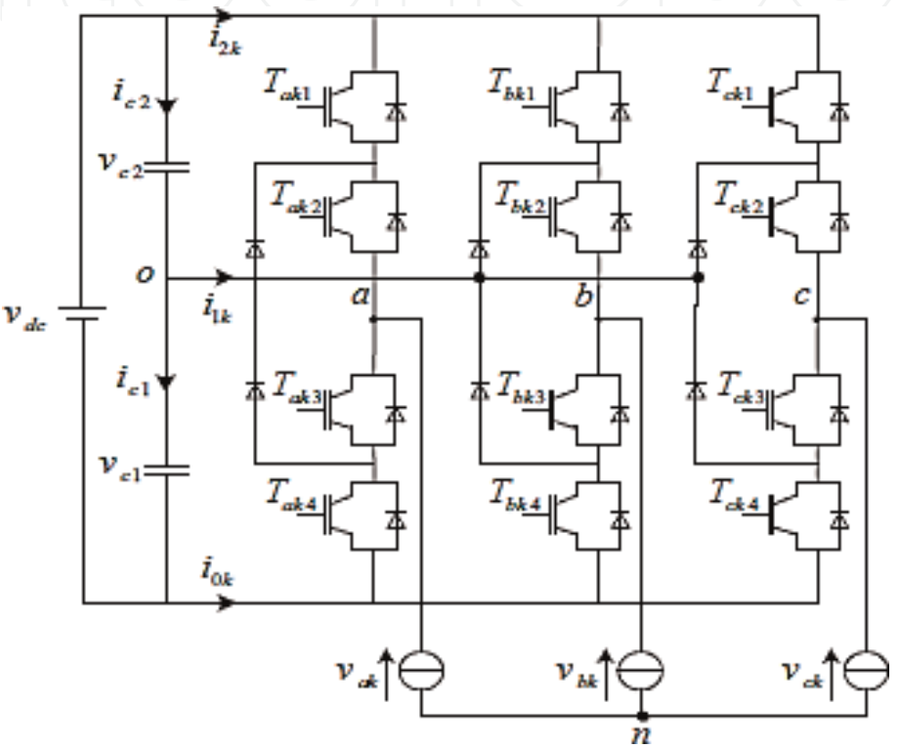

Figure 1.
Three-phase inverter with floating diodes (k = 1 is the first inverter, and k = 2 is the second inverter).

Switching states	State of the switches of an arm				Output voltage
	T_{xk1}	T_{xk2}	T_{xk3}	T_{xk4}	
2	1	1	0	0	v_{c2}
1	0	1	1	0	0
0	0	0	1	1	$-v_{c1}$

Table 1.
States of an arm of the inverter with three levels.

4. Modeling of five-level inverter

Currently the diode-clamped inverter is the one that attracts the most attention, given the simplicity of its structure compared to floating capacity inverters and cascading. In fact, compared to the inverter with floating capacities, it is not necessary to use capacities for each phase, which eliminates the risks of parasitic resonances.

The main advantage lies in a considerable reduction in switching losses and its ability to control harmonic content [13].

Figure 2 shows the structure of the inverter with five levels, each of the three arms of the inverter consists of eight controlled switches and six floating diodes. The controlled switches are unidirectional in voltage and bidirectional current; it is conventional associations of a transistor and an antiparallel diode.

These switches must not be opened or closed simultaneously, in order to avoid a short circuit of the DC source in the input. The floating diodes (six per arm) ensure the application of the different voltage levels at the output of each arm. The DC input voltage is divided into four equal parts using four capacitors [14].

The DC input bus is composed of four capacitors (C1, C2, C3, and C4), making it possible to create a set of three capacitive middle points. The total voltage of the DC bus is v_{dc}; under normal operating conditions, this is uniformly distributed over the four capacitors, which then have a voltage $v_{dc}/4$ at their terminals [15] (**Table 2**).

For each switch T_{xki} (k = 1, 2, i = 1 ... 8, x = a, b, and c), a switching function is defined as follows:

$$F_{xki} = \begin{cases} 1 \; if \; T_{xki} \; is \; ON \\ 0 \; if \; T_{xki} \; is \; OFF \end{cases} \tag{8}$$

The switch control of the lower half-arms is complementary to those of the upper half-arms:

$$F_{xki} = 1 - F_{xk(i-4)} \tag{9}$$

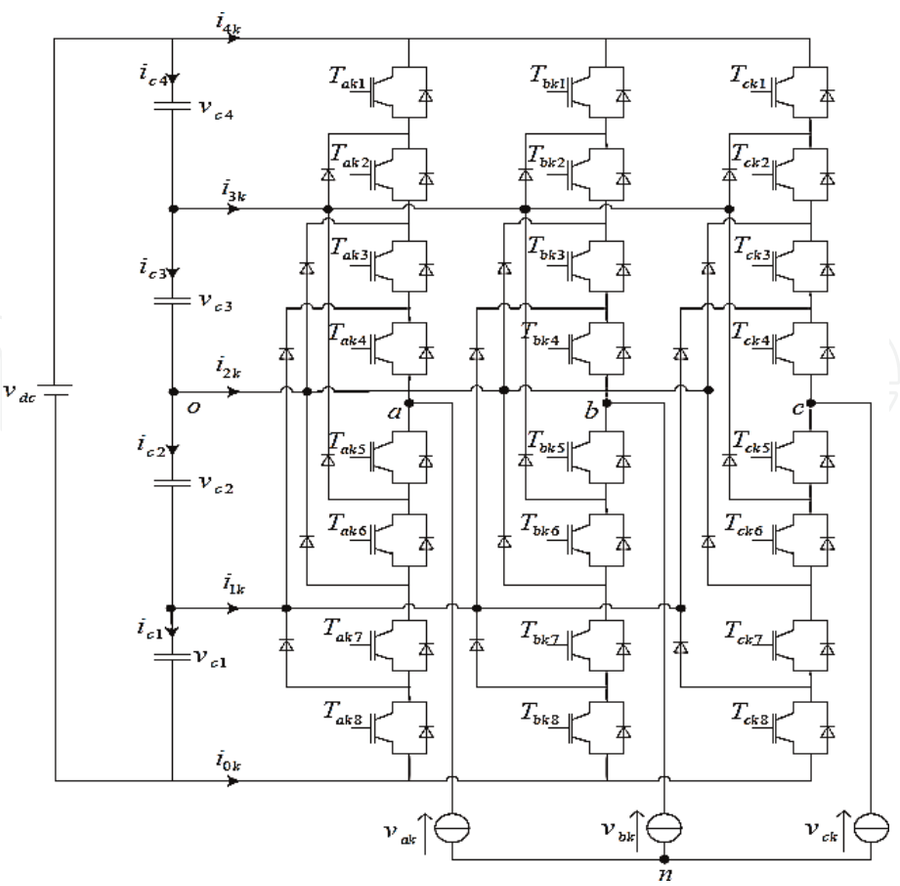

Figure 2.
Diagram of the five-level inverter with NPC structure.

Switching states	State of the switches of an arm								Output voltage
	T_{xk1}	T_{xk2}	T_{xk3}	T_{xk4}	T_{xk5}	T_{xk6}	T_{xk7}	T_{xk8}	
4	1	1	1	1	0	0	0	0	$v_{c3} + v_{c4}$
3	0	1	1	1	1	0	0	0	v_{c3}
2	0	0	1	1	1	1	0	0	0
1	0	0	0	1	1	1	1	0	$-v_{c2}$
0	0	0	0	0	1	1	1	1	$-(v_{c1}+ v_{c2})$

Table 2.
States of an arm of the inverter with five levels.

We define five connection functions, each associated with one of the five states of the arm:

$$\begin{cases} F_{c1xk} = F_{c1xk}F_{c2xk}F_{c3xk}F_{c4xk} \\ F_{c2xk} = F_{c2xk}F_{c3xk}F_{c4xk}F_{c5xk} \\ F_{c3xk} = F_{c3xk}F_{c4xk}F_{c5xk}F_{c6xk} \\ F_{c4xk} = F_{c4xk}F_{c5xk}F_{c6xk}F_{c7xk} \\ F_{c5xk} = F_{c5xk}F_{c6xk}F_{c7xk}F_{c8xk} \end{cases} \tag{10}$$

The potentials of nodes a, b, and c of the three-phase inverter at five levels with respect to the point o are given by the following system:

$$\begin{pmatrix} v_{a0k} \\ v_{b0k} \\ v_{c0k} \end{pmatrix} = \begin{pmatrix} F_{c1ak} & F_{c2ak} & F_{c3ak} & F_{c4ak} & F_{c5ak} \\ F_{c1bk} & F_{c2bk} & F_{c3bk} & F_{c4bk} & F_{c5bk} \\ F_{c1ck} & F_{c2ck} & F_{c3ck} & F_{c4ck} & F_{c5ck} \end{pmatrix} \begin{pmatrix} v_{c3} + v_{c4} \\ v_{c3} \\ 0 \\ -v_{c2} \\ -(v_{c1} + v_{c2}) \end{pmatrix} \tag{11}$$

5. Direct torque control based on neural networks

The direct torque control of a DSIM is based on the direct determination of the control sequence applied to the switches of a voltage inverter. This choice is based generally on the use of hysteresis comparators whose function is to control the state of the system, namely, the amplitude of the stator flux and the electromagnetic torque [16].

In the structure of the DTC, the voltage model is commonly used. Thus, the amplitude of the stator flux is estimated from its components following the axes (α, β):

$$\begin{cases} \hat{\phi}_{\alpha s} = \int_0^t (V_{\alpha s} - R_s I_{\alpha s})dt \\ \hat{\phi}_{\beta s} = \int_0^t (V_{\beta s} - R_s I_{\beta s})dt \end{cases} \tag{12}$$

The stator flux module is given by

$$\hat{\varphi}_s = \sqrt{\hat{\varphi}_\alpha^2 + \hat{\varphi}_\beta^2} \tag{13}$$

The angle θ_s is given by

$$\hat{\theta}_s = \tan 2^{-1}\left(\frac{\hat{\varphi}_\beta(t)}{\hat{\varphi}_\alpha(t)}\right) \tag{14}$$

This method of estimating the stator flux has the advantage of simplicity and accuracy, particularly at medium and high speeds where the ohmic voltage drop becomes negligible [17].

The electromagnetic torque can be estimated from the estimated magnitudes of the stator flux and the measured magnitudes of the line currents, by the following equation:

$$\hat{T}_{em} = \frac{3}{2}p.\left(\hat{\phi}_{\alpha s} i_{\beta s} - \hat{\phi}_{\beta s} i_{\alpha s}\right) \tag{15}$$

5.1 Neural network strategy

The human brain is able to adapt, learn, and decide, and it is on this fact that researchers have been interested in understanding its operating principle and being able to apply it to the field of computer science.

Among the disadvantages of DTC control, a slow response for small changes in stator flux and electromagnetic torque, size, and complexity of switching tables when the number of levels of inverters is high. In order to improve the performance of the DTC control, many contributions have been made in the DTC control based on artificial neural networks [18].

In this application, our goal is to replace switching tables with artificial neural networks.

The multilayer architecture was chosen to be applied to multilevel DTC control. This network, which can be multiplexed for each controller output, has acceptable performance in many industrial applications [19]. The neural network contains three layers: input layer, hidden layers, and output layer. Each layer consists of several neurons. The number of neurons in the output and the layers depends on the number of input and output variables chosen. The number of hidden layers and the number of neurons in each one depend on the dynamics of the system and the desired degree of accuracy.

Figure 3 shows the structure of the neural network applied to the multilevel DTC control of the DSIM. It is a network with three neurons in the input layer, whose inputs are flow error (Ef), torque error (Ec), and flow position angle (Z) [20]. For the three-level inverter, there are 12 neurons in the hidden layer and 06 neurons in the output, and for the five-level inverter, there are 24 neurons in the hidden layer and 12 neurons in the output. **Figure 4** shows the chosen architecture.

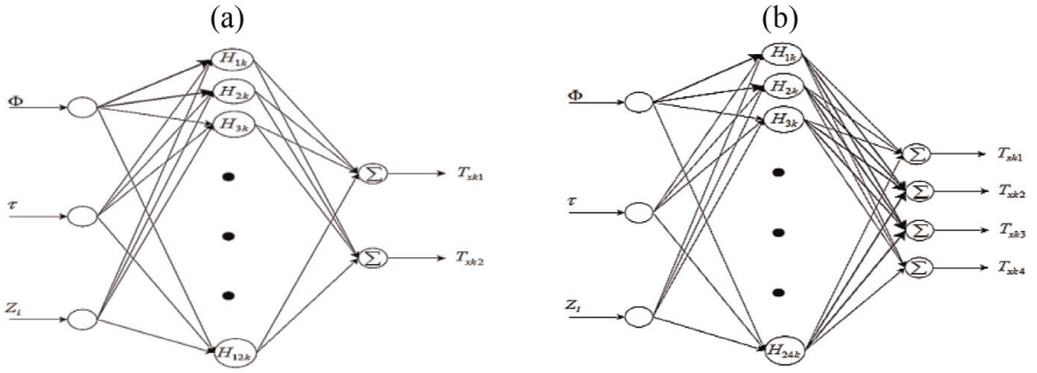

Figure 3.
Neural network structure applied to the multilevel DTC control. (a) for three-level DTC, (b) for five-level DTC.

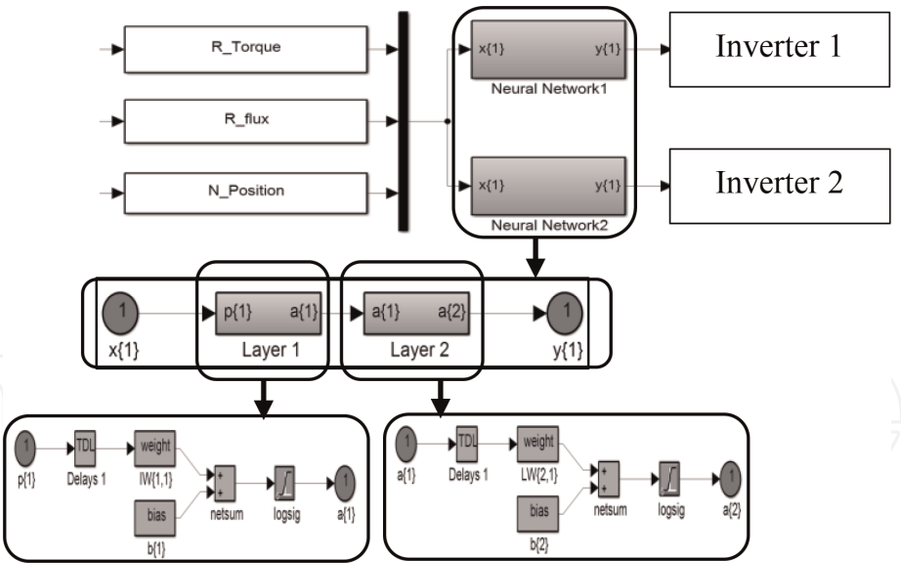

Figure 4.
Selection table based on neuron network.

6. Simulation results

In order to test the static and dynamic performance of the control, the DSIM is accelerated from standstill to reference speed 100 rad/s. The machine is applied

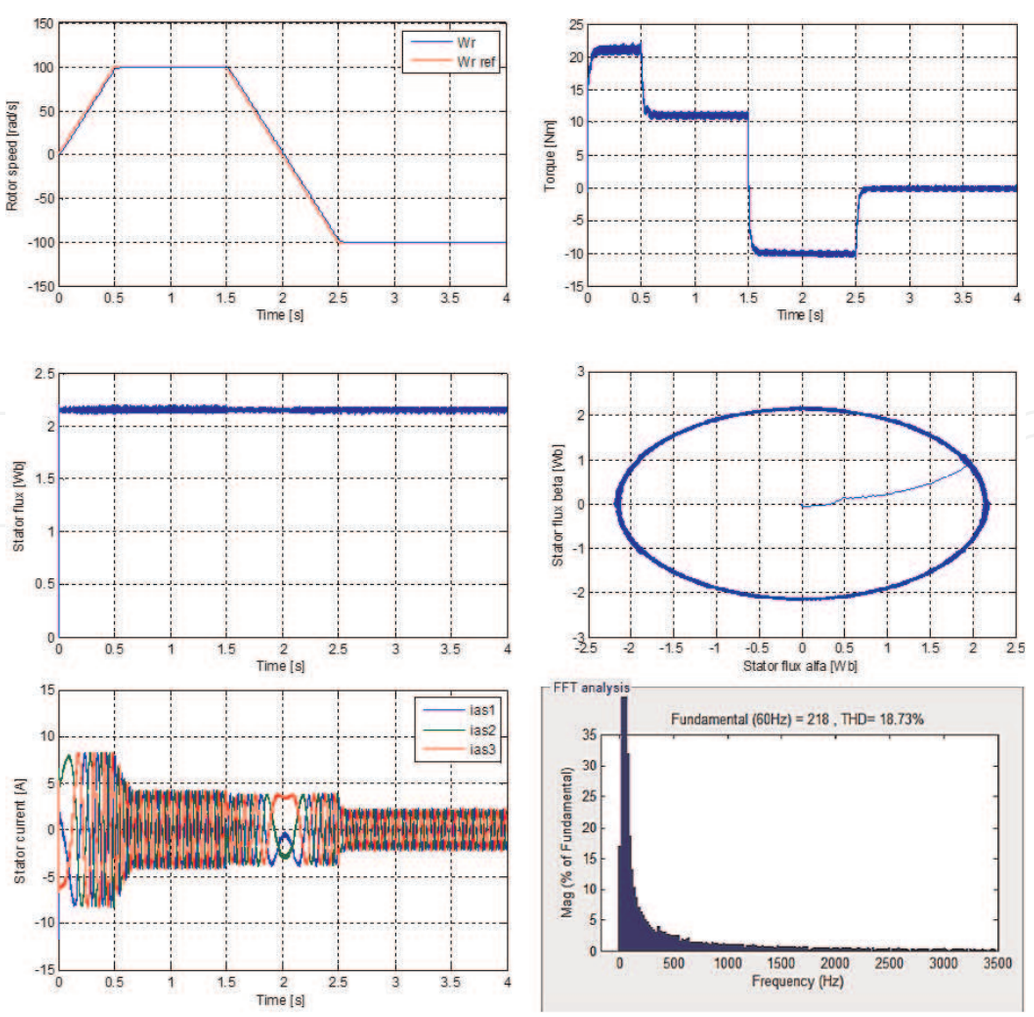

Figure 5.
Simulation results of real and estimated speed, torque, flux, and current of three-level DTC-ANN.

with a load torque of 11 Nm. Finally, the direction of rotation of the machine is reversed from 100 rad/s to −100 rad/s at time t = 2 s. **Figures 5** and **6** show the simulation results of the three- and five-level DTC control for DSIM.

Simulation results of speed, stator flux, torque, stator current, and stator voltage show the good performance of the three- and five-level DTC-ANN control of DSIM (speed, stability, and precision).

We note that the speed follows its reference value. The electromagnetic torque stabilizes at the value of the nominal torque after a transient regime with rapid response and without exceeding before stabilizing at the value of the applied load torque.

Figure 6 shows that the five-level DTC-ANN control reduces the ripple of the electromagnetic torque, the stator flux, and the THD value compared to that of the three-level DTC-ANN. On the other hand, we note that the speed reaches its reference without exceeding for the two control types. Moreover, the couple follows the load torque. The dynamics of the stator flux are not affected by the application of these load instructions.

The use of multilevel inverter at five levels causes a decrease in the current ripple at the steady state that is to say low peaks than that of the three-level control. However, the results of the simulations shows a good dynamic characteristic of the stator flux in the transient regime for five-level DTC-ANN compared to the three-level DTC-ANN with static errors that are virtually null in both cases of control DTC proposed.

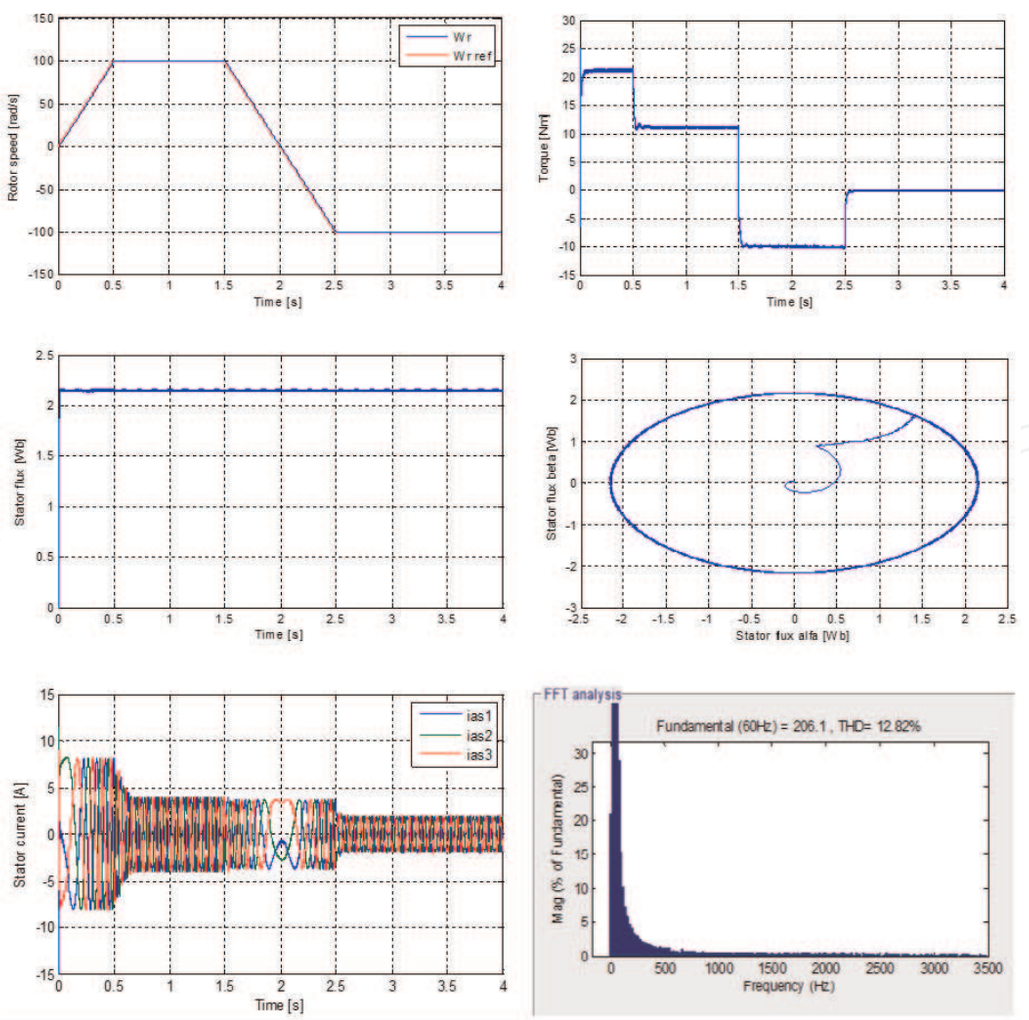

Figure 6.
Simulation results of real and estimated speed, torque, flux, and current of five-level DTC-ANN.

Figures 7 and **8** show the simulation results of the three-level and five-level DTC-ANN control for low-speed operation. DSIM is accelerated from standstill to a low reference speed of 10 rad/s, at time t = 0.5 s; the DSIM is accelerated again to a reference speed of 100 rad/s. The machine is loaded with a nominal load of 11 Nm. Finally, a reversal of the direction of rotation of the machine from 100 rad/s to −10 rad/s is performed at time t = 2 s.

The simulation results show that low-speed operation does not affect the performance of the proposed drive. Indeed, the good reference speed tracking is ensured, with advantages brought by the use of five-level DTC-ANN control, the minimization of torque ripple, and stator flux, which is confirmed by the simulation results.

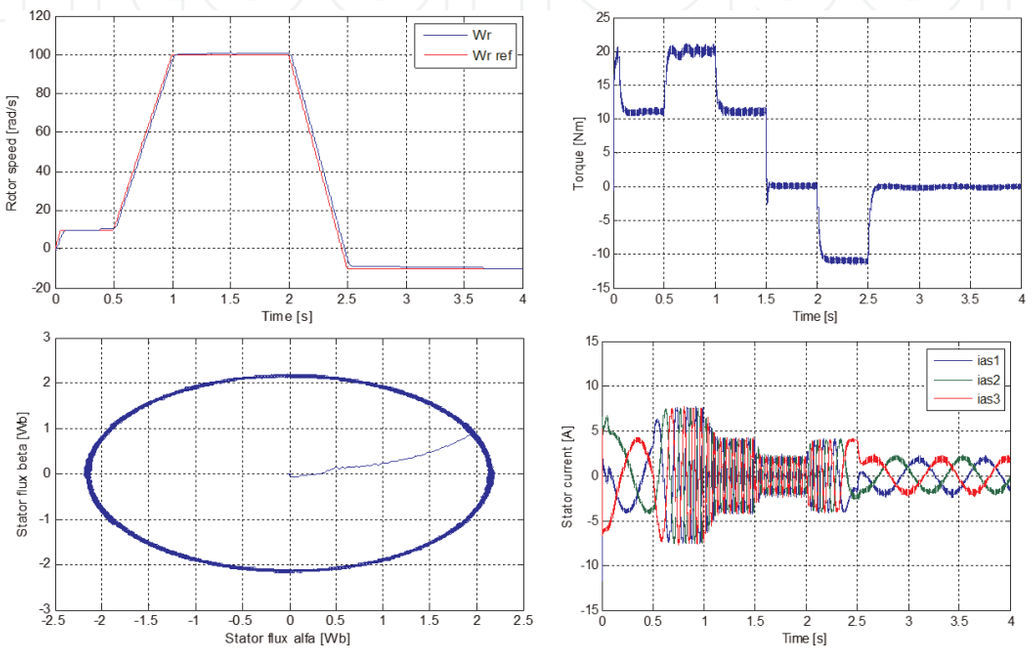

Figure 7.
Simulation results of three-level DTC-ANN for low-speed operation.

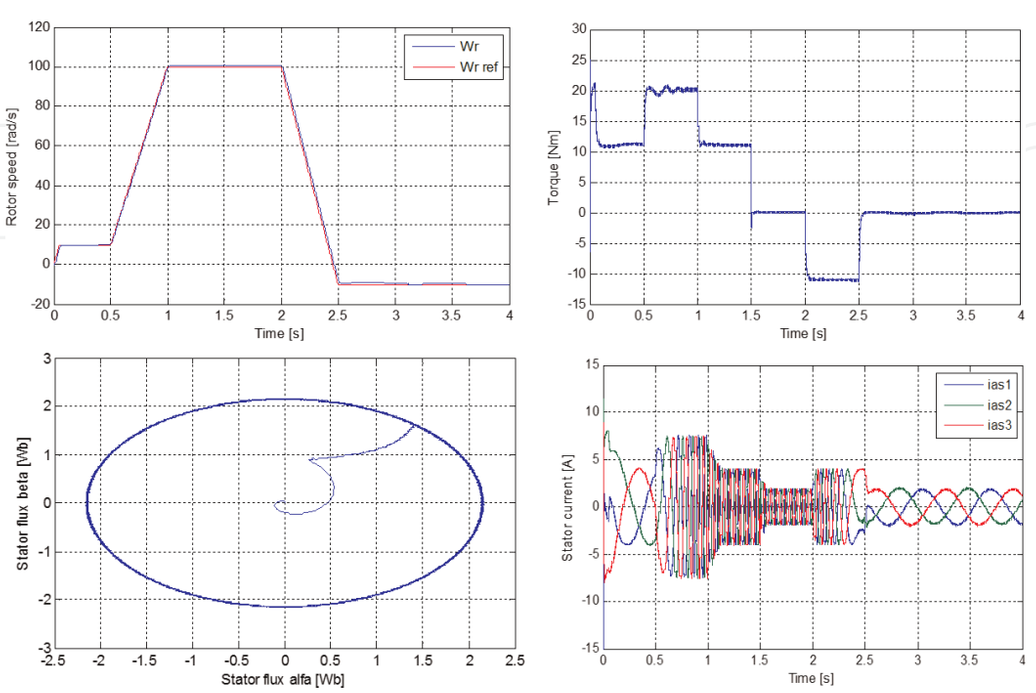

Figure 8.
Simulation results of five-level DTC-ANN for low-speed operation.

	THD (%)	Ripples of torque	Ripples of flux
Three-level DTC	18.73	Good	Good
Five-level DTC	12.82	Very good	Very good

Table 3.
The comparison between three-level and five-level DTC-ANN.

In order to know the best type control of DSIM, a comparative study is essential between the two types (three-level DTC-ANN and five-level DTC-ANN). The following table shows the comparison between the two types (**Table 3**).

7. Conclusion

In this chapter, we presented two types of DTC control (three-level DTC-ANN and five-level DTC-ANN) of a DSIM fed by two NPC voltage inverters, and the technique of neural networks was applied to the DTC control. The main advantage of this control is to allow control of the flux and torque of the machine without the need to use a mechanical sensor. The direct torque control strategy is an effective and simple way to control an induction machine. In order to improve the performance of the DSIM (torque ripple reductions, flux, response time, and the THD value of the stator current), simulation tests of the control by variation and inversely of the speed have been presented; the results obtained show that the five-level DTC-ANN control with speed control is very efficient. This shows the effectiveness of the proposed strategy.

Appendix

DSIM parameters

P_n = 4.5 Kw
I_n = 6 A
R_r = 2.12 Ω
L_r = 0.006 H
$R_{s1} = R_{s2}$ = 1.86 Ω
$L_{s1} = L_{s2}$ = 0.011 H
L_m = 0.3672 H
J = 0.065 kg.m^2
k_f = 0.001 Nm/rad.

IntechOpen

Author details

Mohamed Haithem Lazreg* and Abderrahim Bentaallah
Faculty of Electrical Engineering, Laboratory of Intelligent Control and Electrical power Systems (ICEPS), Djillali Liabes University of Sidi Bel Abbes, Algeria

*Address all correspondence to: haitem.31@hotmail.fr

IntechOpen

References

[1] Kirankumar B, Reddy YV, Vijayakumar M. Multilevel inverter with space vector modulation: Intelligence direct torque control of induction motor. IET Power Electronics. 2017;**10**:1129-1137

[2] Nabae A, Takahashi I, Akagi H. A new neutral-point-clamped PWM inverter. IEEE Transactions on Industrial Applications. 1981;**IA-17**: 518-523

[3] Babaei E, Dehqan A, Sabahi M. A new topology for multilevel inverter considering its optimal structures. Electric Power Systems Research. 2013; **103**:145-156

[4] Gupta K, Bhatnagar P. Chapter 2 – Basics of multilevel inverters. In: Multilevel Inverters Conventional and Emerging Topologies and their Control; 2018. pp. 21-42

[5] Meroufel A, Massoum S, Bentaallah A, et al. Double star induction motor direct torque control with fuzzy sliding mode speed controller. Revue Roumaine des Sciences Techniques - Serie Électrotechnique et Énergétique. 2017; **62**:31-35

[6] Taheri A. Harmonic reduction of direct torque control of six-phase induction motor. ISA Transactions. 2016;**63**:299-314

[7] Khedher A, Mimouni MF. Sensorless-adaptive DTC of double star induction motor. Energy Conversion and Management. 2010;**51**:2878-2892

[8] Gadoue SM, Giaouris D, Finch JW. Artificial intelligence-based speed control of DTC induction motor drives — A comparative study. Electric Power Systems Research. 2009;**79**:210-219

[9] Lazreg MH, Bentaallah A. Speed sensorless vector control of double star induction machine using reduced order observer and MRAS estimator. In: IEEE International Conference on Electrical Engineering (ICEE-B); Boumerdes, Algeria; 2017

[10] Lazreg MH, Bentaallah A. Sensorless fuzzy sliding-mode control of the double-star induction motor using a sliding-mode observer. Elektrotehniški Vestnik. 2018;**85**:169-176

[11] Payami S, Behera RK, Iqbal A. DTC of three-level NPC inverter fed five-phase induction motor drive with novel neutral point voltage balancing scheme. IEEE Transactions on Power Electronics. 2018;**33**:1487-1500

[12] Harina MM, Vanithaa V, Jayakumar M. Comparison of PWM techniques for a three level modular multilevel inverter. Energy Procedia. 2017;**117**:666-673

[13] Figarado S, Sivakumar K, Ramchand R, Das A, Patel C, Gopakumar K. Five-level inverter scheme for an open-end winding induction machine with less number of switches. IET Power Electronics. 2010;**3**: 637-647

[14] Rosmadi A, Nasrudin A, Siti R, Sheikh R, Zaharin A. A five-level diode-clamped inverter with three-level boost converter. IEEE Transactions on Industrial Electronics. 2014;**61**: 5155-5163

[15] Naganathan P, Srinivas S, Ittamveettil H. Five-level torque controller-based DTC method for a cascaded three-level inverter fed induction motor drive. IET Power Electronics. 2017;**10**:1223-1230

[16] Talaeizadeh V, Kianinezhad R, Seyfossadat SG, Shayanfar HA. Direct torque control of six-phase induction motors using three-phase matrix

converter. Energy Conversion and Management. 2010;**51**:2482-2491

[17] Usta MA, Okumus HI, Kahveci HA. Simplified three-level SVM-DTC induction motor drive with speed and stator resistance estimation based on extended Kalman filter. Electrical Engineering. 2017;**99**:707-720

[18] Barika S, Jaladi KK. Five-phase induction motor DTC-SVM scheme with PI controller and ANN controller. Procedia Technology. 2016;**25**:816-823

[19] Zolfaghari M, Taher SA, Munuz DV. Neural network-based sensorless direct power control of permanent magnet synchronous motor. Ain Shams Engineering Journal. 2016;**7**:729-740

[20] Douiri MR, Cherkaoui M. Comparative study of various artificial intelligence approaches applied to direct torque control of induction motor drives. Frontiers in Energy. 2013;**7**: 456-467